Light Metals 2011 *Edited by: Stephen J. Lindsay*
TMS (The Minerals, Metals & Materials Society), 2011

Investigation of heat transfer conditions in a reverberatory melting furnace by numerical modeling

Andreas Buchholz[1], John Rødseth[2]
[1]Hydro Aluminium Rolled Products GmbH, R&D, P.O. Box 2468, D-53014 Bonn, Germany
[2]Hydro Aluminium as, R&D Materials Technology, Karmøy, N-4265 Håvik, Norway

Keywords: melting, reverberatory furnace, numerical modeling

Abstract

A numerical model based on the commercial software ANSYS FLUENT was used to analyze the heat transfer conditions in an industrial reverberatory melting furnace. The model comprises different physical phenomena as gas flow, chemical reactions, i.e. combustion, conduction, radiation and latent heat release in the metal. The gas circulation was analyzed for different metal loads and burner arrangements. The melting process inside the furnace is inherently time-dependent, and a complete transient analysis is very time-consuming. To study the impact of varied burner positions on the energy utilization, stationary solutions were applied, where the effect of melting heat was approximated by artificial heat sinks inside the metal. The results of the stationary solutions were compared with fully transient results to guarantee the transferability of the cost-efficient steady state calculations. The results stress the dominant effect of radiative heat transfer in the melting process.

Introduction

Rising energy prices, the economic crisis, national commitments for carbon footprint reductions and the need for a better image of the aluminium industry have put a constant pressure to reduce energy consumptions in casthouses worldwide, but especially in Europe. Since the resources for new investments are limited, the existing casthouses have to achieve energy savings by moderate modifications of existing equipment and improved procedures in the operations.

In recent years Hydro Aluminium R&D has developed a furnace model to analyze impacts of furnace operations on melt quality [1][2]. Since this model covers all essential heat transfer mechanisms required to describe the heat flow in a reverberatory furnace, it was decided to investigate the melting process in an existing melting furnace and to analyze various options to improve the utilization of the fuel energy.

The furnace has a nominal capacity of 35 t and is run in a batch mode. About 20 t of aluminium are charged as cold metal and later 12 t as potroom metal. The rest is the heel of the previous melting process. The furnace is heated by two cold air burners with a nominal power of 2.5 MW and 1.0 MW.

The study should answer, what factors dominate the heat transfer, whether a modified burner position could achieve a better utilization of fuel energy and how the metal charging and burner operation could be optimized to reduce the fuel consumption.

Numerical model

The furnace model is based on the commercial software ANSYS FLUENT 12.1. The model covers the following physical phenomena:

1. gas flow
2. combustion (chemical reaction)
3. heat conduction and advection in the gas
4. heat conduction in the metal and the walls
5. radiation
6. heat of fusion.

The gas flow is modeled as incompressible turbulent flow using the RNG version of the K-epsilon model. The mixing rates calculated in the turbulence model are the basis to model the chemical reactions of the combustion process. This so-called Eddy-Dissipation model assumes a fast chemistry, where the speed of reaction is exclusively determined by the turbulent mixing rate. The oxidation of natural gas is approximated by a simplified 2-step reaction scheme for methane gas decomposition:

(1) $CH_4 + 1\ ½\ O_2 \Rightarrow CO + 2\ H_2O$
(2) $CO + ½\ O_2 \Rightarrow CO_2$

For each chemical component in the reaction scheme an individual transport equation has to be solved.

The radiation is calculated with the so-called Discrete Ordinate approach, where radiation transfer equations are solved for a finite number of space angles in each computational cell. Besides calculating the radiation between surfaces this model is also capable to capture absorption effects of radiative gas components.

To account for heat of fusion, a latent heat term was implemented into the heat transport equation by user defined functions, since FLUENT's built-in solidification model is not compatible with the combustion model. The latent heat was introduced as an effective specific heat into the temperature formulation [3] of the heat transport equation. Specific measures guarantee that no latent heat is lost in the iteration process. The model was validated in experiments in a lab scale furnace [4].

One major limitation of the model at the moment is that the metal shape will not change during the melting process. Therefore, redistribution of the liquid metal will not be described fully correctly. To encompass the consequences of this shortcoming, two different metal arrangements were considered. In the first configuration the metal is considered as a melt pool spread at the bottom of the furnace cavity, in the second version the metal is arranged as an ingot assembly including gaps, which allow for the circulation of combustion gases between the ingots and thus increasing the effective metal surface.

Furnace geometry

The furnace geometry was strongly simplified. Details of the steel construction were neglected. To capture heat capacity effects of

the refractory material the walls were modeled as thick walls. In the original configuration the 2.5 MW burner is opposite to the front door and the smaller 1.0 MW burner left hand of the door. Figures 1 and 2 show the two basic cases of this study. Figure 1 assumes that 20t of metal are spread at the bottom of the furnace, in Figure 2 the same amount of metal is arranged as a stack of 27 ingots. The majority of the geometry was meshed using tetrahedral cells and later converted into a polyhedral mesh. The final meshes consisted of about 450000 cells and 2 million nodes.

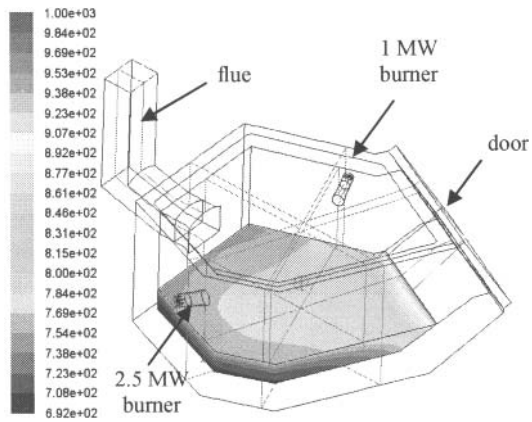

Figure 1. Melt pool configuration A: 20 t of metal spread at the bottom of the furnace. The colors represent temperatures in °C.

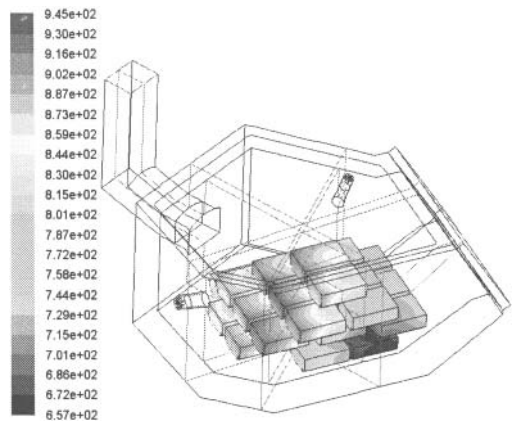

Figure 2: Ingot arrangement, configuration B: 20 t of metal distributed as a stack of 27 ingots.

Besides the two different metal distributions several modifications of burner positions were investigated. The main idea was to find a configuration with a longer residence time of the combustion gases. It was assumed that the extended residence time could lead to a higher fraction of energy transferred to the metal. The options to find a reasonable burner arrangement are limited. Besides the original configuration one promising approach seemed to place the burners to the flue side. An overview of the different arrangements and development of the related gas flow patterns is shown in Figure 3.

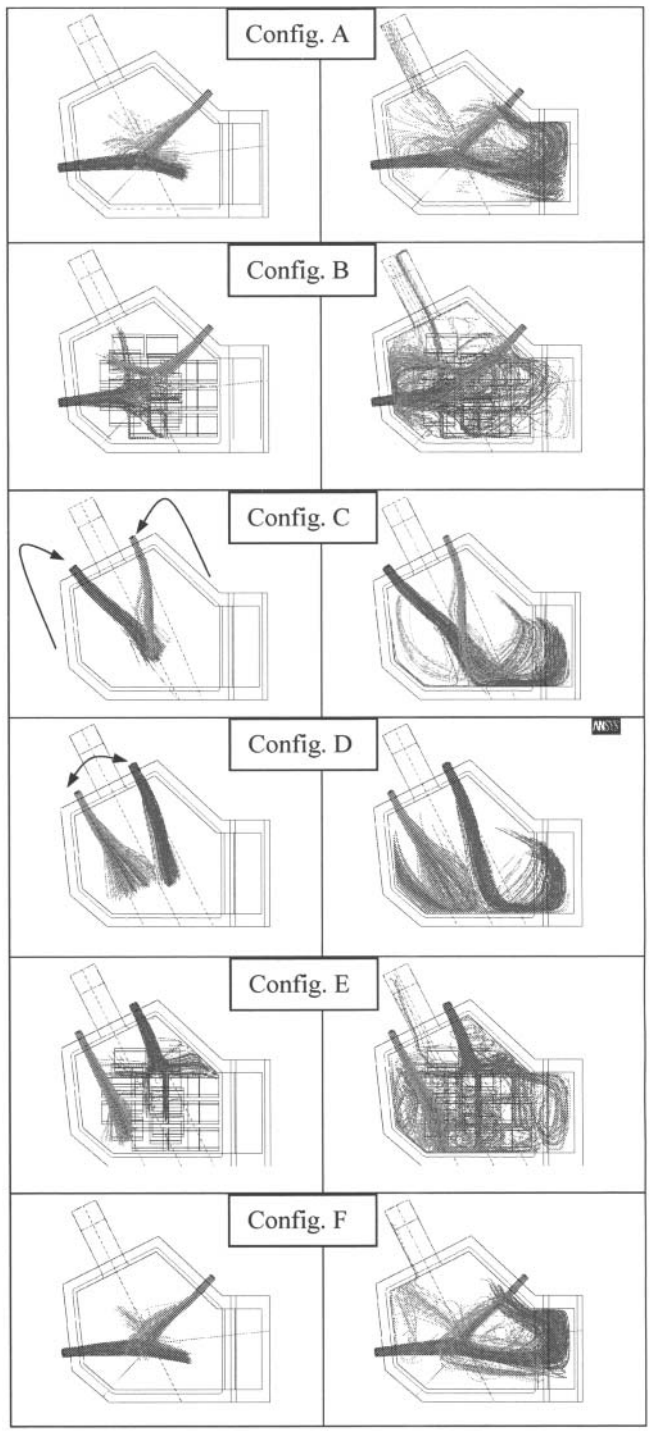

Figure 3. Overview of investigated furnace configurations and development of flow patterns. Blue pathlines are generated by the 2.5 MW burner, the orange patterns by the 1.0 MW.

Configuration A and B represent the original furnace layout, in A the metal is spread at the furnace bottom as shown in Figure 1, while in B an ingot stack as in Figure 2 is considered. In configuration C the burners were shifted to the flue side. In this setup the larger burner was slightly tilted towards the furnace center. Since the further flow pattern showed an overweight of gas circulation close to the front door, this setup was further developed into configuration D: The 2.5 MW burner and the 1.0 MW burner were exchanged at their positions and adjusted to be parallel to the flue axis. This measure provided a more uniform circulation pattern. Finally, this burner arrangement D was applied to the ingot stack, as shown in configuration E. The geometry in configuration F is identical to A. The only difference is a changed composition of the oxidizer to imitate oxy-fuel burners, as will be discussed later.

Steady state calculations

The flow patterns shown in Figure 3 are generated from steady state calculations, since it turned out that fully transient calculations of a complete melting cycle are very time consuming and costly. When calculating the steady state of a furnace running with burners at melting power the solution will finally show a completely superheated furnace with an unrealistic temperature distribution. The steady state solution needed in this work should resemble a snapshot somewhere in the middle of a transient melting process. Therefore, it was necessary to place an artificial heat sink into the metal, which imitates absorption of heat of fusion in the real transient process. It was assumed that an appropriate description of a volumetric heat sink term in the metal can be provided by a formula of the type:

$$Q = - \alpha_{Sink} (T - T_{Ref}) \qquad (1)$$

The advantage of this formula is that the metal temperature can be used as an indicator to compare the efficiency of heat transfer conditions in different setups. A higher average metal temperature would point out a more efficient furnace configuration. Some estimates based on the real melting performance and subsequent adjustments lead to the following choice of heat sink parameters, which were used throughout the steady state calculations: $\alpha_{Sink} = 355$ J/(m^{3}s) and $T_{Ref} = 500$°C.
It was assumed that this heat sink together with identical boundary conditions could provide the means to calculate temperatures and heat flux distributions of the different geometric configurations, which can be used to compare the relative performance of the different setups.

Transient calculations

To assess how far the steady solutions are in agreement with a fully transient analysis, configurations A and B were calculated as transient cases. These simulations were based on previous steady state solutions, but the temperature values of the metal were re-initialized to 20 °C. The artificial heat sink term in the metal was switched off, while the transient latent heat term was activated. Table I gives an overview of typical thermo-physical data and process parameters used in the steady state and transient calculations. To avoid over-prediction of the temperatures in the combustion gas a modified polynomial description of gas specific heats was used as recommended in the FLUENT documentation [5]. The composition of the natural gas was assumed to be 86% methane, 1% carbon dioxide and 13% nitrogen.

Table I. Thermo-Physical Data and Process Parameters

Property/Parameter	Value	Unit
aluminium density	2350	kg/m^3
aluminium specific heat	1080	J/(kg K)
aluminium heat conductivity	200	W/(m K)
aluminium emissivity	0.3	
aluminium latent heat of fusion	390000	J/kg
refractory density	2320	kg/m^3
refractory specific heat	1138	J/(kg K)
refractory heat conductivity	0.5	W/(m K)
refractory emissivity	0.6	
air flow, 1 MW burner	1200	m^3/h
natural gas flow, 1 MW burner	100	m^3/h
air flow, 2.5 MW burner	1970	m^3/h
natural gas flow, 2.5 MW burner	170	m^3/h
computed combined burner power	2.3	MW

Figure 4 shows a comparison of average metal and flue gas temperatures and of the average fraction liquid of the transient calculations of configurations A and B.

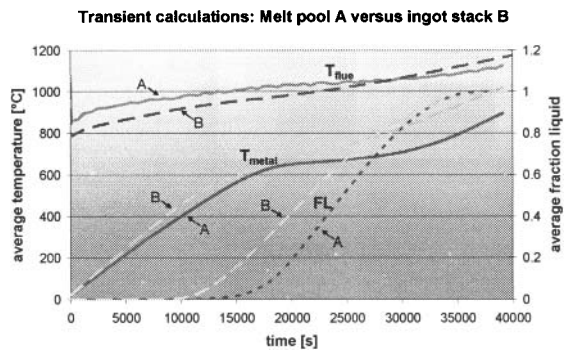

Figure 4. Results of transient calculations of configurations A (melt pool) and B (ingot stack): Average flue gas temperatures (orange/red), average metal temperatures (light green/dark green) and average fraction liquid (light blue/blue).

The average temperature of the ingot stack is always ahead of the melt pool configuration. This is a consequence of the increased specific metal surface of the ingot stack, the direct impact of the flame onto some ingots and the circulation of the combustion gases between the ingots. Therefore, the metal starts earlier to melt and the flue gas temperature is lower – at least in the beginning – compared to the melt pool. After about 20000s this situation changes: the melting of the melt pool is accelerating and finally the average fraction liquid catches up with the ingot stack at 33000s. Finally, the fully liquid state is reached slightly earlier (after 37965s) than in the ingot arrangement (39720s). This result appears to be unrealistic, especially since the average temperature of the ingot stack is still higher. It follows from the model limitation that all metal stays in its initial location and cannot flow away after melting. Finally some parts of the stack are very hot, while other regions are shielded from the direct impact of burner the burner flame and remain comparatively cold. In this respect conclusions have to be made with care from the computed data at the end of the melting process. Generally, it can be concluded that the ingot stack exhibits more favorable heat transfer conditions compared to the melt pool configuration.

When integrating the fuel flow until the fully liquid state is achieved, a specific melting energy can be calculated for both configurations. The melt pool calculation yields a value of 1200 kWh/t versus 1295 kWh/t for the ingot stack. This compares rather well to the typical value of 1200 kWh/t which is usually reported for cold burner installations. Actually the calculated specific consumption may be even too pessimistic. Since certain areas of the metal are very much superheated, when the last solid fraction is molten, the complete melting could have probably been achieved, even when the burner power had been reduced earlier and superheat utilized for melting of the remaining solid.

One question, which should be answered by the transient calculations, was how much the earlier described steady state computations are representative for the complete transient melting process. When comparing average flue gas and average metal temperatures of transient and steady state calculations it turns out that they match at different times (see Figure 5). When the flue gas temperatures are identical at about 26000s, the metal temperature of the steady state solution is about 70 K higher than in the transient solution. A better match could have been probably achieved when choosing lower values of α_{Sink} and T_{Ref} in equation (1).

Nevertheless, looking at the heat fluxes it can be noticed that the total, radiative and convective heat fluxes through the metal – gas interface are very similar for both the steady state solution and a broad period of time in the transient solution (see Figure 6). It is very remarkable that the radiative component of the heat flux dominates the heat transfer between gas and metal by far.

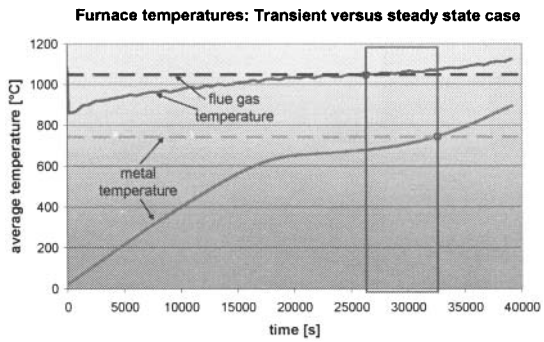

Figure 5. Comparison of steady state solution (horizontal lines) and transient solution of melt pool arrangement A.

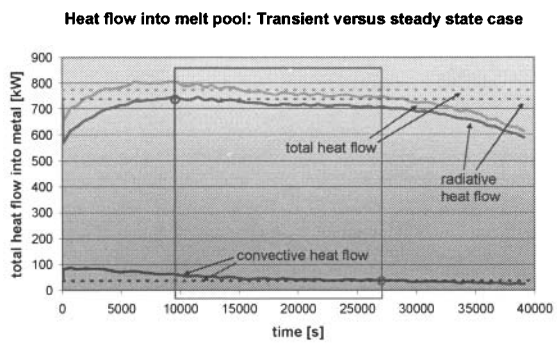

Figure 6. Comparison of heat flow (total, convective and radiative contributions) through gas – metal interface in steady state (horizontal lines) and transient calculation of melt pool configuration A.

Comparison of heat transfer conditions in steady state calculations

The reasonable agreement of heat fluxes in steady state and transient calculations justifies the usage of the heat fluxes as a criterion to compare the efficiency of heat transfer conditions in the steady state calculations of the different configurations shown in Figure 3. An overview of the total heat flows is given in Figure 7. As mentioned earlier, configuration F uses the same geometry as A, but the composition of the combustion air was changed to imitate oxy-fuel burners.

It turns out that the shift of the burners from the side walls to the flue side in configurations C and D has virtually no benefit compared to the original layout A. The increased effective surface area of the ingot stack implies some small gain in total heat flow in configurations B and E. On the other hand, it is remarkable that the average heat flux (heat flow per area) of these configurations is significantly reduced as shown in Figure 8.

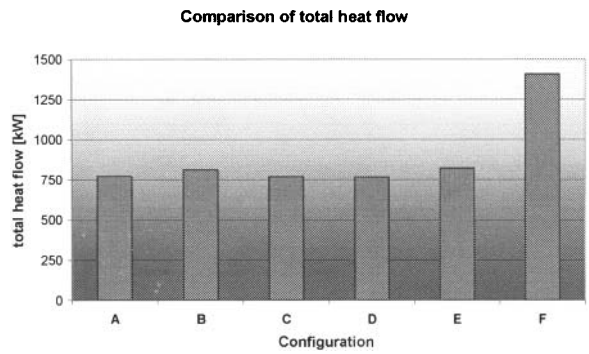

Figure 7. Comparison of total heat flow into the metal in steady state calculations of the configurations shown in Figure 3.

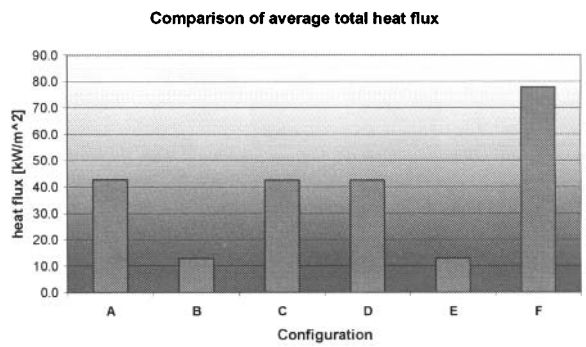

Figure 8. Average heat flux through the metal surface of configurations A – F shown in Figure 3.

Most outstanding is the behavior of the imitated oxy-fuel configuration F, which reveals superior heat transfer properties. Several factors are responsible for this advantage:

1. Effectively, the nitrogen was removed from the oxidizer. This means that less gas volume needs to be heated. The flame gets hotter.
2. A hotter flame can emit more heat by radiation. It was noticed earlier that radiation is the dominant effect in the heat transfer mechanisms and will take full advantage of a temperature increase.

3. A higher fraction of combustion gases consists of radiative components CO_2 and H_2O, which will facilitate the distribution of heat.
4. Due to the reduced amount of oxidizer the combusted gases remain longer inside the furnace and have more time to yield heat.

The last item can be clearly seen in an analysis of gas residence times of the considered configurations, see Figure 9. In this context it is also remarkable that the ingot stack cases B and E also show a significantly increased average residence time. It seems that the impact of the metal stack is less to reflect the gas towards the flue than to divert it from a regular pattern. The diverted combustion gases remain longer inside the furnace.

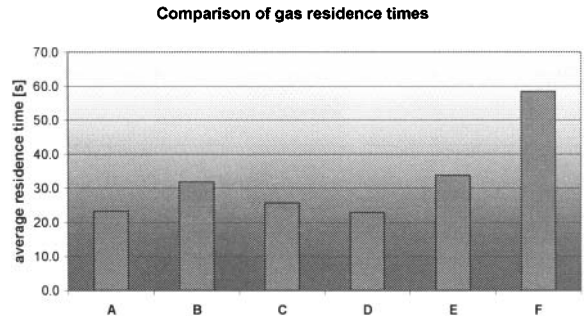

Figure 9. Average gas residence times of the configurations A – F.

Optimization of charging schemes and burner operation

As mentioned in the introduction a part of the metal is added as superheated liquid potroom metal. An interesting question is when the liquid metal should be added to utilize both the better heat transfer conditions of the initial ingot stack and the superheat from the potroom metal. In this scope it is important to measure the amount of energy, which is really transferred to the metal. The average temperature and the average fraction liquid as shown in Figure 1 are not helpful. It is more convenient to look at the average enthalpy density of metal inside the furnace (see Figure 10). In this diagram the former time axis is now converted into an energy axis by multiplication with the burner power. The enthalpy density covers sensible heat and heat of fusion. It is interesting to see that the average enthalpy density curves of the melt pool and of the ingot stack do not differ very much.

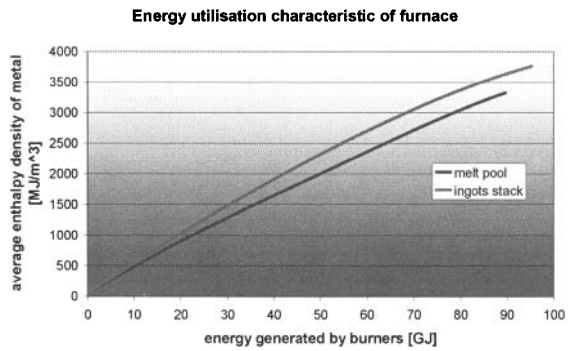

Figure 10. Average enthalpy density of metal inside the furnace depending on consumed energy.

One attractive option to optimize the fuel consumption could be to assume a unified energy transfer curve to control the heat content, burner operation and addition of liquid metal, see Figure 11 (green line). The actual state of the metal inside the furnace is described by point A on the conversion curve. The target value for metal transfer is represented by point C. The superheated potroom metal has a enthalpy value B further up on a curve. By weighing with the different metal amounts it can be calculated that the potroom metal together with the furnace metal would reach the target value C, if the furnace metal were at point D. Thus the difference of point A and D on the x-axis gives the remaining amount of energy, which still has to be generated by the burners. Knowing the actual burner power the remaining up-time of the burner can be calculated easily.

At the moment production data of flue, roof and metal temperature are analyzed to investigate the feasibility of this kind of control scheme in the real installation.

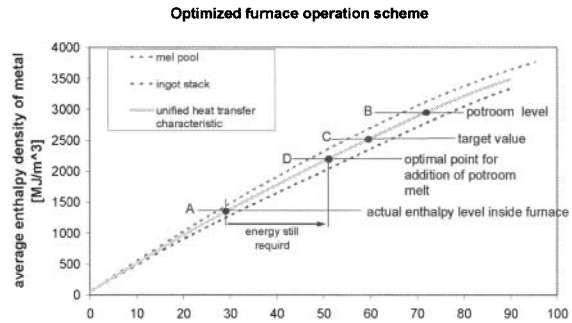

Figure 11. Control scheme to optimize liquid metal addition and burner operation.

Conclusions

A numerical furnace model was successfully applied to analyze the heat transfer conditions in a reverberatory melting furnace.

- It turned out that the heat transfer is by far dominated by radiation effects.
- Due to the approximately spherical shape of the furnace, modifications of the burner positions showed almost no improvements concerning gas residence times and energy utilization. The potential to achieve energy reductions by this kind of modifications seems to be limited.
- A more promising approach to improve the heat transfer inside the furnace could be the application of oxy-fuel burners. Of course, the much higher efficiency has to be weighed against the additional costs for the oxygen supply.
- Considering different metal distributions inside the furnace, it can be noticed that the heat transfer into an ingot stack is higher than into a melt pool.
- It is recommended to heat the ingots as long as possible and add liquid metal not before the optimal amount of energy was brought into the cold metal.
- A timing scheme for the burners based on the heat transfer characteristics inside the furnace could be used to control and minimize the amount of energy, which is transferred into the metal.

Acknowledgments

The authors would like to thank casthouse manager Pål T. Endresen and the crew of Hydro Aluminium Karmøy Rolling Mill for enduring stimulation and support in this project.

Literature

[1] S. Instone, A. Buchholz, G.-U. Grün: TMS Light Metals 2008, 811-816
[2] G.-U. Grün, A. Buchholz, TMS Light Metals 2009, 735-742
[3] V.R. Voller, C.R. Swaminathan, Numerical Heat Transfer B, 19(2), 1991, 175-189
[4] J. Furu, A. Buchholz, T.H. Bergstrøm, K. Marthinsen, TMS Light Metals 2010, 679-684
[5] ANSYS FLUENT 12.0 User's Guide, ANSYS, Inc. 2009, chap. 15.1.3, p 15.24-25